Optical RI sensor based on an in-fiber Bragg grating Fabry-Perot cavity embedded with a micro-channel

Zhijun Yan*, Pouneh Saffari, Kaiming Zhou, Adedotun Adebay, Lin Zhang
Photonic Research Group, Aston University, Birmingham, B4 7ET, UK
Corresponding address: yanz1@aston.ac.uk

ABSTRACT

We report a linear response optical refractive index (RI) sensor, which is fabricated based on a micro-channel created within a Fabry Perot (F-P) cavity by chemical etching assisted by femtosecond laser inscription. The experimental results show the F-P resonance peak has a linear response with the RI of medium and the measuring sensitivity is proportion to the length of micro-channel. The sensor with 5 μm -long micro-channel exhibited an RI sensitivity of 1.15nm/RIU and this sensitivity increased to 9.08nm/RIU when widening the micro-channel to 35μm. Furthermore, such micro-channel FP sensors show a much broader RI sensing dynamic range (from 1.3 to 1.7) than other reported optical fiber sensors.

Keywords: FBG, femtosecond laser, refractive index, micro-channel, F-P sensors

1. INTRODUCTION

Optical fiber based reflective index (RI) sensors are widely applied in chemical/biomedical measurement and environmental monitoring applications, due to their desirable characteristics, such as small size, high sensitivity, immunity to electromagnetic interference and safe-operation for hazardous environmental conditions. Most of fiber based sensors achieved the RI sensing by evanesce field coupling, which is an indirect method [1-4]. The response between the sensing signal and the RI value is nonlinear, and the sensing range is very narrow limited to 1.4 to 1.44. Recently, there are many papers that have presented the novel RI sensors employing serial Fabry-Perot (F-P) interferometer structures [5-10]. These types of sensor have good linear response and large sensing range. There are different methods reported to form fiber based F-P cavity sensors, such as splicing photonic-crystal or multi-mode fiber between two single mode fibers; forming an air-gap between two single mode fibers; creating a micro-cavity in the fiber core by laser machining [9-11]. With the development of femtosencond laser (fs), based on fs micro-machine technique, the researchers have achieved a series of micro-structures in an optical fiber [12]. In our previous works, we have successfully achieved micro-holes and micro-slots in optical fibers by fs laser inscription assisted chemical etching [13-15]. In this paper, we report an F-P cavity formed by UV-inscribing two fiber Bragg grating (FBG) with 1mm gap in a fiber, and created a micro-channel by fs-inscription assisted chemical etching in the middle of the cavity. Such micro-channel F-P structures have been evaluated for RI sensing. It is

Microstructured and Specialty Optical Fibres, edited by Kyriacos Kalli, Alexis Mendez,
Proc. of SPIE Vol. 8426, 842609 · © 2012 SPIE · CCC code: 0277-786X/12/$18 · doi: 10.1117/12.921410

apparent that without micro-channel, the FBG F-P in the fiber core is intrinsically insensitive to the RI of surrounding medium, as the light is screened by the cladding. The embedded micro-channel in the F-P with one dimension across the whole fiber section will give an access to the surrounding liquid to the F-P structure, thus causing cavity property change. In our initial experiment, two sensors with different length micro-channel sizes (5μm and 35μm) have been investigated in RI sensing experiment.

2. Measuring principle and fabrication

The configuration of FBG F-P cavity based RI sensor is shown in Fig. 1, which has a micro-channel of a length L embedded into an F-P cavity that is formed by a pair of FBGs with the same central wavelength in the fiber core and separated by a distance of L1. The micro-channel is along the fiber axis with lateral dimension slightly larger than the diameter of the fiber core, so that the whole fiber core area has been removed, which could make sure the wave front of the light is not distorted and scattered greatly when propagating in the channel region.

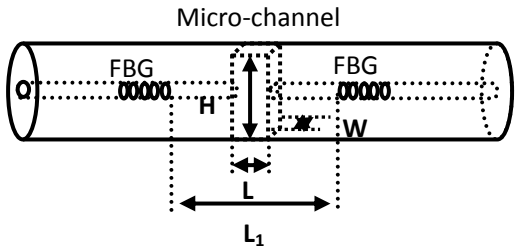

Figure 1 the schematics of the Fiber Bragg Grating Fabry Perot RI sensor with a micro-channel embedded in the middle, W, H and L are the width, height and length, respectively.

According to the theory [16], the propagation phase shift Φ induced by an F-P cavity in our design includes two parts: one is induced by the fiber core cavity with constant index; the other is induced by the surrounding medium with variable index. The expression could be defined as:

$$\Phi = \frac{4\pi\left[n_{fibercore}(L_1 - L) + n_{surrounding}L\right]}{\lambda} \quad (1)$$

Where nfibercore is the effective refractive index of fiber core, L1 is the separation distance of two FBGs, L is the length of micro-channel, λ is the free-space wavelength and nsurrounding is the refractive index of surrounding medium. When the phase shift is 2mπ (where m is an integer), the reflection is the maximum. The corresponding wavelength λm for the F-P reflection peak is expressed by:

$$\lambda_m = \frac{2\left[n_{fibrecore}(L_1 - L) + n_{surrounding}L\right]}{m} \quad (m=\pm1,2,3\ldots) \quad (2)$$

By differentiating equation 2 (here, L1, L and nfibercore are all constants, only the nsurrounding is variable), the wavelength shift can be expressed as a function of the perturbation of reflective index of the micro-channel:

$$\partial\lambda_m = \frac{2L}{m}\partial n \tag{3}$$

From equation 3, it clearly shows that the former is linearly in response to the latter and the RI sensitivity is directly in proportion to the length of micro-channel. And the RI sensitivity is inverse proportion to the order m. As can been seen in later section, these principles are also verified in our experimental results.

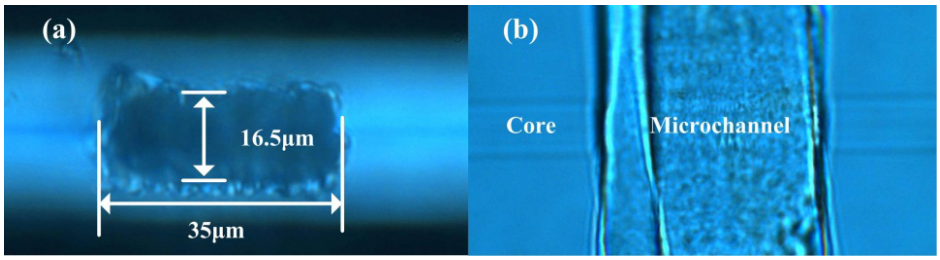

Figure 2 the micro-images of micro-channel fabricated by fs laser inscription assisted chemical etching process: (a) micro-channel on the surface of fiber showing the channel length of ~35μm and width of ~16.4μm; (b) micro-channel across whole fiber section

By the UV inscription technique, two 3dB-FBGs with ~1551nm operating wavelength were written into the fiber with 1mm-long gap, which formed a 1mm long F-P cavity, and a micro-channel was fabricated in the middle of the cavity by fs laser inscription assisted chemical etching. The fabrication process of the micro-channel involved two main steps: (1) Inscription of the designed structure into the fiber by using a tightly focused fs laser beam; (2) Etching the fiber in a solution of 5% hydrofluoric acid (HF) for selective removal of the fs laser modified region. During the laser inscription process, the fs laser pulses (center wavelength=800 nm) were focused into the silica fiber by using a 100×objective lens with a NA of 0.55 and a working distance of 13 mm. The laser pulse width was measured to be 150 fs, and the repetition rate was at 1 kHz. The focused spot size was evaluated to be 1.5μm, and the average pulse energy was measured to be 550nJ. The Fig. 2 shows the microscope images of micro-channels fabricated by fs laser. We can see clearly the width of channel (16.4 μm) is larger than the diameter of the fiber core (~10 μm for SMF 28) , and the whole core has been removed, after chemical etching.

Two samples with different micro-channel lengths (5μm and 35μm) were fabricated. Fig.3 shows the transmission spectral evolution of the FBG F-P sensors from post-UV-inscription to fs-inscription,

chemical etching and immersing in RI solution. The two FBGs were UV-inscribed with 3dB strength and the top plots in Fig. 3 show the spectra of the FBG F-P cavities with 5μm and 35μm micro-channel lengths. Both plots exhibit typical F-P resonance feature with two transmission passbands generated within the original Bragg reflection band in ~1551nm region. As shown from the second and third plots in the figure, after fs laser inscription and chemical etching, the F-P resonant peaks are shifted due to the refractive index change in the micro-channel area. Note, when the micro-channel created, the average index of the cavity is reduced as the micro-channel region is filled in with air. We noticed that the FBG F-P with 35μm micro-channel induced much higher insertion loss (about 15dB) than ~2.5dB of 5μm one and its transmission passband feature also disappeared as shown in 3rd plot of Fig. 3(b). However, when the micro-channels were filled with solutions, the F-P resonance feature recovered and the resonances shifted to the longer wavelength side, as shown in the last plots of Fig. 3.

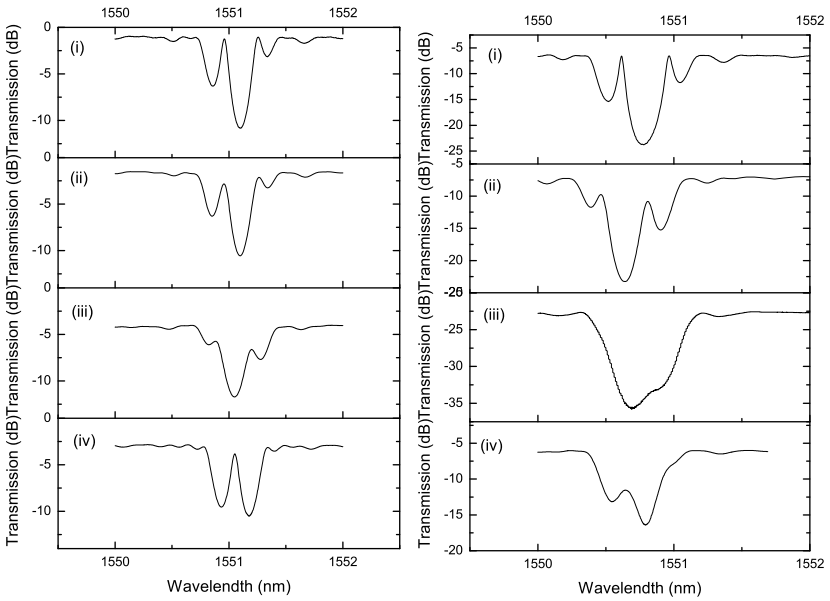

Figure 3 The transmission spectra of FBG F-P sensors of (a) 5μm and (b) 35μm micro-channels. (i): before fs laser modified; (ii): after fs inscription; (iii): afer chemical etching and micro-channels created; (iv): when the 5μm micro-channel filled in with RI=1.306 and 35mm with RI=1.428 solutions.

3. Experimental results and discussion

To evaluate the RI sensing capability of the FBG F-P sensor embedded with micro-channel, we apply a series of index oils (from Cargille laboratory) to measure the response of micro-channel FBG F-P devices to RI. In the experiment, in order to observe clearly the shift of the resonant peaks, we set the resolution of optical spectra analyzer (OSA) at 0.01 nm and the wavelength scanning range at 3 nm, and kept the devices at room temperature during the measuring process. After each measurement, the device was rinsed with methanol to remove the residual oil in the micro-channel till the original

spectrum in air is restored. The shift of wavelength was almost instantaneously observed during the measurement, when the index oil infused into the micro-channel.

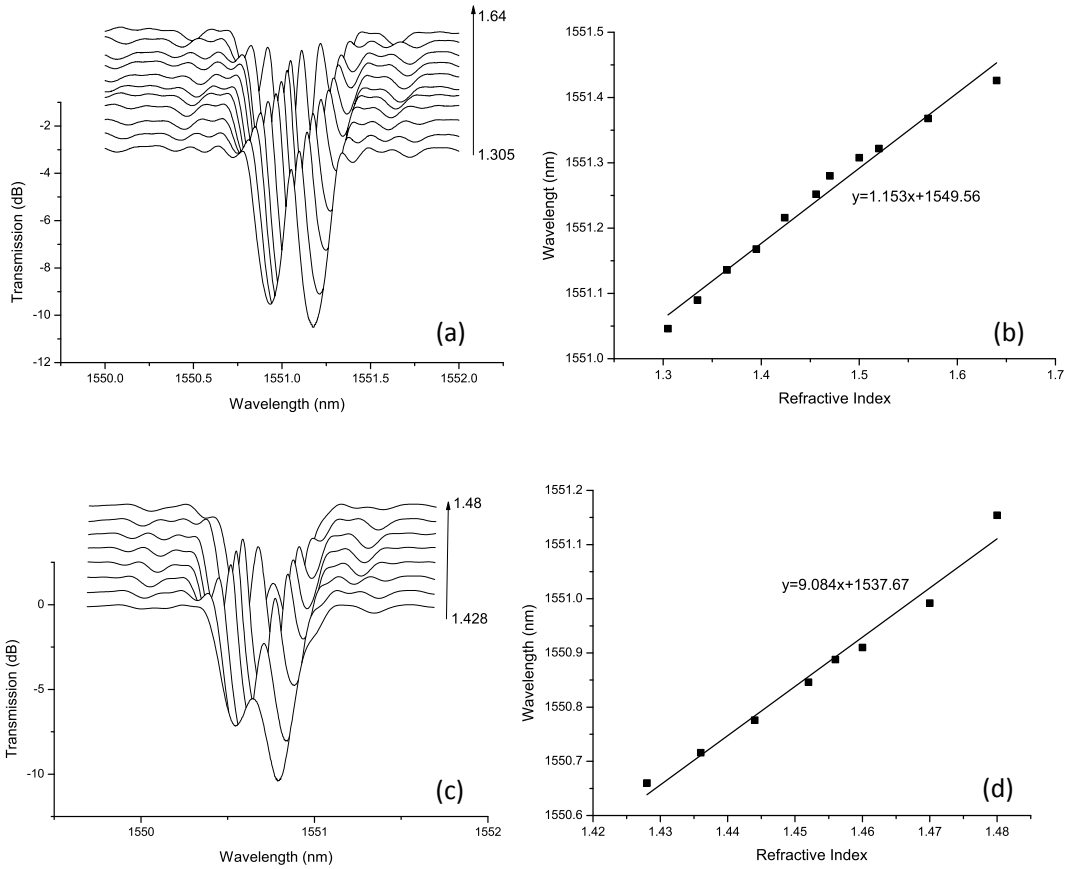

Figure 4 Spectra of the (a) 5Õm (c) 35µm micro-channel devices submerged in different RI oils. Linear relation plots between the wavelength of the resonant peak and RI of the oil, with a coefficient of 1.153nm/RIU for (b) 5mm and 9.084/RIU for (d) 35 µm micro-channel devices.

Fig. 4(a) shows the spectra of the 5Õm micro-channel sample with increasing RI. It can be seen the F-P resonant peaks shift from the shorter to longer wavelength side with increasing RI and eventually move out of the Bragg reflection band, while the higher order peaks are regenerated from the shorter wavelength side. The relation of the peak wavelength with respect to RI for the 5Õm micro-channel FBG FP is given in Fig. 4 (b), showing a linear trend with an RI sensitivity about 1.1nm/RIU (refractive index unit). Noticeably, this narrow micro-channel FBG F-P device can detect RI change in a wide range from 1.306 up to 1.7, which is remarkably higher than all fiber grating based RI sensors, which usually only sensitive from 1.4 to .44 region. For the 35Õm micro-channel sample, the results show the sensitivity is 9.085nm/RIU (see Fig. 4 (d)), which is almost nine times higher than the 5µm micro-channel one, but its sensing range is much narrower available only from 1.43 to 1.49 (see Fig. 4 (c)). That is because the high loss at the small RI makes the FP resonances very weak, and the

resonant peak move quickly out of the Bragg reflection band due to the high sensitivity. In general, the bandwidth of FBG is around 0.5 nm. For 1.1nm/RIU sensitivity, the sensing range would be ~0.45 RIU and for 9.085 nm/RIU, the sensing range is reduced to ~0.055 RIU. Thus, there is a trade-off between the RI sensitivity and sensing range for micro-channel FBG F-P sensor, and the best performance sensor can be achieved by design the micro-channel size to suit the application. By comparing the performance of these two micro-channel FBG F-P devices, we can see that the wider micro-channel sample gives a much higher RI sensitivity, which is in excellent agreement with the principle shown in equation 4. However, the wider channel causes the higher insertion loss that limits the sensing range and S/N. In contrast, the narrower channel sample exhibits low insertion loss and works for a much broader RI sensing range but with lower sensitivity.

4. Conclusions

We have successfully created a micro-channel in an FBG based F-P cavity by fs laser inscription assisted chemical etching and proposed this structure as an RI sensor. The experimental results show this type of sensors owns a good linear RI response. Two micro-channels with different widths (5μm and 35μm) were investigated for RI sensing. They both show good linear RI response with sensitivities of 1.15nm/RIU and 9.08nm/RIU, respectively. The narrow channel device gives a much larger RI sensing range from 1.3 to 1.7. Although the broader channel device can work only in a limited RI range from 1.43 to 1.49, due to considerable high loss in low RI and narrow Bragg reflection band, it exhibited RI sensitivity nine times higher than the narrow micro-channel sensor. The revealed linear RI response with significantly larger detection range is of great advantage over fiber grating based RI sensors, as that all have a nonlinear RI response with detection range limited to fiber core index 1.44. With these remarkable advantages, micro-channel FBG F-P structures can be further developed into high performance bio/chemical/environmental sensors.

5. References

[1] J. Yang, *et al.*, "Long-period grating refractive index sensor with a modified cladding structure for large operational range and high sensitivity," *Appl. Opt.,* vol. 45, pp. 6142-6147, 2006.

[2] X. Wu, *et al.*, "Refractive index sensor based on surface-plasmon interference," *Opt. Lett.,* vol. 34, pp. 392-394, 2009.

[3] A. Iadicicco, *et al.*, "Thinned fiber Bragg gratings as high sensitivity refractive index sensor," *Photonics Technology Letters, IEEE,* vol. 16, pp. 1149-1151, 2004.

[4] Y. H. Wei Liang, Yong Xu, Reginald K. Lee, and Amnon Yariv, "Highly sensitive fiber Bragg grating refractive index sensors," *Applied Physics Letters,* vol. 86, p. 3, 2005.

[5] W. Zhou, *et al.*, "Compact refractometer based on extrinsic-phase-shift fiber Bragg grating," *Sensors and Actuators A: Physical,* vol. 168, pp. 46-50, 2011.

[6] Y. Jinpeng, *et al.*, "Highly Sensitive Refractive Index Optical Fiber Sensors Fabricated by a Femtosecond Laser," *Photonics Journal, IEEE,* vol. 3, pp. 1189-1197, 2011.

[7] Y. Wang, *et al.*, "Fiber in-line Mach-Zehnder interferometer fabricated by femtosecond laser micromachining for refractive index measurement with high sensitivity," *J. Opt. Soc. Am. B,* vol. 27, pp. 370-374, 2010.

[8] T. Wei, *et al.*, "Temperature-insensitive miniaturized fiber inline Fabry-Perot interferometer for highly sensitive refractive index measurement," *Opt. Express,* vol. 16, pp. 5764-5769, 2008.

[9] G. Xiao, *et al.*, "Fiber Optic Fabry-Perot Interferometric Gas Pressure Sensors Embedded in Pressure Fittings," *Microwave and Optical Technology Letters,* vol. 42, pp. 486-489, 2004.

[10] R. Zengling, *et al.*, "A Miniature Fiber-Optic Refractive-Index Sensor Based on Laser-Machined Fabry Perot Interferometer Tip," *Lightwave Technology, Journal of,* vol. 27, pp. 5426-5429, 2009.

[11] R. Jha, *et al.*, "Refractometry based on a photonic crystal fiber interferometer," *Opt. Lett.,* vol. 34, pp. 617-619, 2009.

[12] R. R. Gattass and E. Mazur, "Femtosecond laser micromachining in transparent materials," *Nat Photon,* vol. 2, pp. 219-225, 2008.

[13] Y. Lai, *et al.*, "Microchannels in conventional single-mode fibers," *Opt. Lett.,* vol. 31, pp. 2559-2561, 2006.

[14] K. Zhou, *et al.*, "A refractometer based on a micro-slot in a fiber Bragg grating formed by chemically assisted femtosecond laser processing," *Opt. Express,* vol. 15, pp. 15848-15853, 2007.

[15] H. Fu, *et al.*, "Microchanneled Chirped Fiber Bragg Grating Formed by Femtosecond Laser-Aided Chemical Etching for Refractive Index and Temperature Measurements," *Photonics Technology Letters, IEEE,* vol. 20, pp. 1609-1611, 2008.

[16] S. G. L. Lipson, H.; Tannhauser, D.S., " Optical Physics (3rd ed.)," *London: Cambridge U.P.,* 1995.